Mapping the Hidden Universe: The Universe Behind the Milky Way – The Universe in H I
ASP Conference Series, Vol. 3×10^8*, 2000*
R. C. Kraan-Korteweg, P. A. Henning, and H. Andernach, eds.

IR-TF Relation In The Zone Of Avoidance With 2MASS

N.Bouché & S.Schneider
The University of Massachusetts, Dpt of Astronomy, Amherst, MA 01003 USA

Abstract. Using the Tully-Fisher relation, one can map the peculiar velocity field and estimate the mass in regions such as the Great Attractor. 2MASS is surveying the full sky in J, H and K bands and has the great advantage that it allows us to detect galaxies more uniformly to lower Galactic latitude than optical surveys. This study shows the feasibility of using 2MASS and the TF relation to probe large scale structure. We found that (i) we can use axis ratio b/a up to 0.5; (ii) intrinsic extinction is present (up to 0.5mag at J, 0.1 mag at K); (iii) the zero-point of the TF relation is independent of the 2MASS magnitude measurement and is consistent with the HST Key-Project value; (iv) the 2MASS K-band 20th mag/arcsec^2 isophotal aperture magnitude produces the best TF relation; and (v) there is no type dependence of the residuals.

1. Introduction. The Tully-Fisher relation

In 1977, Tully and Fisher (hereafter TF; Tully & Fisher 1977) discovered that there is a good correlation between maximum rotational velocity, usually given by the global neutral hydrogen line profile width ΔV[1] and the absolute magnitude M for late-type galaxies.

Observationally, the correlation (luminosity vs. maximum velocity) gives $L \propto \Delta V^{\alpha}$ with α in the range of 2.5-3 at optical wavelengths. There is a general trend that at longer wavelengths, the slope steepens. At infrared wavelengths, the slope ($-2.5 \times \alpha$ in magnitude) climbs to about -10 (or $\alpha \sim 4$) which is close enough to the Faber-Jackson $L \propto \sigma_v^4$ to suspect a possible common physical origin.

The origin of the TF relation lies (in the very roughest terms) in the virial theorem. Assuming a constant mass-to-light (M/L) ratio and constant surface brightness (I), one can rewrite the virial theorem as

$$L \propto V^4[(M/L)^2 I]^{-1} \tag{1}$$

The zero-point b is directly related to basic physical properties as it can be seen if rewritten as $-2.5 \times \log[I(M/L)^2]$ or $\log[(M/L)\Sigma]$. Σ is the surface mass density which is a strong function of the angular momentum ($\Sigma \propto M^7/J^4$) whereas the mass-to-light (M/L) gives information on the stellar content. This can be used

[1] corrected for inclination.

to put strong constraints on galaxy formation theory (see Steinmetz & Navarro 1999; Koda et al 1999).

Zwaan et al. 1995 also have shown that low surface brightness (LSB) late-type galaxies follow the same B-band TF relation as the HSB, even though their mass-to-light ratios are very different as well as the ratio of dark to luminous matter (de Blok & McGaugh 1997), but this is still somewhat controversial (see O'Neil et al 2000).

The HST Key Project group on the extra-galactic scale have used the TF relation to infer the Hubble constant (H_o) (see Sakai et al 1999 for a recent discussion). Another application is to use the TF to measure the peculiar velocity field of galaxies. This provides an estimate of the mass density on large scales and of the density of the universe through $\Omega^{0.6}/b$.

Using near-IR for TF studies has two advantages: (1) it is sensitive to old red stars and less sensitive to young blue stars. In other words, it is fairly independent of current star formation, so it provides a measure of current stellar content that is, presumably, more closely tied to the total mass of the galaxy and hence its kinematics. (2) Uncertainties due to interstellar absorption in both our own Galaxy and in the observed galaxy are greatly reduced.

This project shows the feasibility of using 2MASS (Huchra et al 2000; Jarrett et al 2000) and HI data to study large scale structure. We studied the Pisces-Perseus (PP) super-cluster region and the GA in the Zone Of Avoidance. In particular, we ask the following questions regarding 2MASS:

(i) Which band (J, H or K) generates the best TF relation?

(ii) What magnitude measurement give the tightest TF relation?

(iii) Can we use 2MASS data at low Galactic latitude?

and regarding the TF relation:

(iv) What is the highest axis ratio b/a that we can use?

(v) Is there any internal extinction?

The remainder of this paper is organized as follow. In section 2, we present our data sets. The method is described in section 3. Our results are presented in section 4 and summarized in section 5.

2. Data sets

We construct two data sets. The first (PP) data set consists of HI data selected from the Huchtmeier & Richter catalog (HR) (Huchtmeier & Richter 1989). Because we found substantial scatter was introduced when using line widths measured in different ways, we select only papers with Giovanelli and collaborators. The data was also restricted to the Arecibo telescope and measurements made at 50% of the peak. The sample contains $\sim$ 2700 objects. We cross-matched 2MASS data with the Giovanelli subsample. There were 502 matches as of Spring 1999 [2]. This sample covers the sky from 0h to 5hr and 15° to 35° in declination which corresponds to the Pisces-Perseus (PP) super-cluster region.

[2]As of January 2000, there are about 3 times more matches, but the analysis is not completed.

We also used HI data from Giovanelli et al 1997 from their extensive survey of the I-band TF in clusters. We again cross-matched this subsample with the 2MASS database and obtained 300 matches from 22 different clusters (hereafter *cluster* sample). We took into account the different offsets from the Hubble flow (col (4) in table (2) of Giovanelli et al 1997) for each cluster. This sample also contains inclination information both from I-band photometry and from 2MASS which enabled us to perform checks on the 2MASS estimate of the axis ratio.

3. Method and Error budget

3.1. Sub-sampling

In most cases, we restrained ourselves to a subsample with the following constraints: (i) axis ratio b/a less than 0.5. The axis ratio we used was the "super coadd" axial ratio b/a (keyword *sup_ba* in 2MASS database) which is determined from the coadded J, H and K images; (ii) HI flux minimum of 1Jy kms^{-1} in order to remove low SNR HI data; (iii) magnitude cutoff of K=13 mag [3]; (iv) excluding S0 and ellipticals. In general, the b/a constraint and HI detection are sufficient to ensure that no ellipticals are in the subsample; (v) redshifts between z_{min} and z_{max} to examine galaxies in different distance ranges.

Figure 1 shows the TF relation for the *cluster* sample.

3.2. Corrections

In order to improve the quality of the TF relation, a number of corrections are usually made for turbulent motion, instrumental broadening, and extinction. These corrections have a number of adjustable parameters that we investigate here to determine which values or methods work best with the 2MASS data.

We have corrected for (i) instrumental broadening following Bottinelli et al (1990) and Giovanelli et al (1997); (ii) for turbulent motion according to the scheme proposed by Tully & Fouqué 1985 [4]; (iii) for inclination, i.e. $v_{rot} = \frac{W_R}{2 \sin i}$ where W_R is the observed velocity width W_{50} corrected for instrumental broadening and i the disk inclination based on the axis ratio b/a from 2MASS; and (iv) for photometric corrections such as the Galactic extinction (from COBE/ DIRBE maps; Schlegel et al 1998) and internal extinction $\Delta m = -\gamma \log b/a$ where γ characterizes the extinction for an highly inclined galaxy [5].

---

[3] in the PP sample, we had a cutoff on the magnitude errors ($\sigma = 0.1$) which corresponds to a cutoff in magnitude of ~ 13 from the dependence of the magnitude errors with magnitude

[4] This correction is also small and did not improve the scatter of the TF relation.

[5] In general, γ can be a function of galaxy luminosity or velocity width (see Sakai et al 1999 and references therein), but we treated it as a constant.

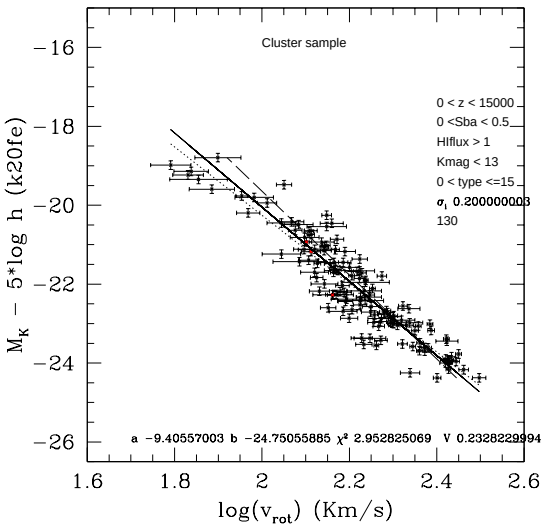

Figure 1. TF relation for a sub-sample (130 objects) of the *cluster* data set with axis ratio $b/a < 0.5$, HI flux > 1 Jy km s^{-1}, magnitude $m_K < 13$ for the I-band sample. The slope a and zero-point b are shown as well as the χ^2_{min} and the variance V. The dotted line is a direct fit, the dashed line is an inverse fit and the bivariate fit is the solid line with an intrinsic scatter σ_i of 0.2 mag. No internal extinction correction was made here.

3.3. Parameterization and Error Budget

We parameterize our TF relation in the same way as Giovanelli et al (1997), $y = a + bx$ where y is the absolute magnitude and x is the logarithm of the rotation velocity, i.e.:

$$x = \log\left[\frac{W_R}{2\sin i}\right] - 2.5 \quad (2)$$

$$y = (m_{obs} - A - \Delta m - k_z - 5\log\frac{cz}{100h} - 25) - 5\log h$$
$$= M - 5\log h \quad (3)$$

where h is the Hubble constant in units of 100 km s^{-1}/Mpc. The last term $-5\log h$ makes y independent of the Hubble constant so it is easier to compare results with other authors. k_z is the k-correction and was generally ignored here since the sample contains only nearby galaxies ($cz < 10000$ km s^{-1}).

A standard χ^2 fit was performed to the data using errors both along the x and y axes, σ_x and σ_y (*bivariate* fit). σ_x includes velocity width uncertainty as well as inclination errors, which dominate the overall error. σ_y includes magnitude uncertainty from 2MASS, distance uncertainty, and an added intrinsic scatter σ_i which takes into account any "cosmological" scatter inherent in the TF relation. The 1σ uncertainty on the parameters (a and b) is given by the projection of the 1σ contour semi-major axis onto the parameter axis (Press et al 1992).

4. Results and discussion

2MASS produces many different magnitude measurements for each objects (Jarrett et al 2000). The different types of magnitude that we used are (i) the 20th mag/arcsec^2 isophotal magnitude (*i20* in 2MASS database [6]); (ii) the 21st mag/arcsec^2 isophotal magnitude (*i21*); (iii) the 20th mag/arcsec^2 K fiducial [7] magnitude (*k20f*); (iv) the 21st mag/arcsec^2 J fiducial magnitude (*j21f*). (v) the Kron (Kron 1980) K fiducial (*kf*) magnitude which measures the flux within an aperture $2r_1$ where r_1 is the first moment of the light distribution. This type of magnitude is thought to be less sensitive to observing conditions and is thought to be a "total" measure of the integrated flux (Koo 1986);

First, which band J, H or K produces the least scatter in the TF relation? Figure 2 shows the minimum value χ^2_{min} of the bivariate fit for each of the magnitude types. Figure 2 indicates that (1) the *20th mag/arcsec^2 K fiducial magnitude* and Kron K fiducial produces the least scatter; (2) in general K gives a tighter TF relation than J or H, considering that H-band photometry of 2MASS is subject to uncertainty due to air glow; (3) Elliptical aperture tend to give a better TF relation than circular ones, although this was not consistently true for all datasets.

Since the different magnitude types have different measurement errors, the χ^2_{min} could look artificially low if the error estimates were inflated. However, we found no effects of this sort. Magnitude types with the largest mean measurement error and it did not produce the smallest χ^2.

Figure 3 shows the fitted values of the slope a and the zero-point b for each of the magnitude types assuming an intrinsic scatter σ_i of 0.2 for the *cluster* sub-sample and using the 2MASS axis ratios for the inclination. First note that the zero-point b of the TF relation is well-determined and does not depend on the magnitude used. Secondly, the slope a is more dependent on the magnitude type. However, the "fiducial" magnitudes are well within 1-σ of each other. Thirdly, the slope a tends to be steeper as the wavelength increases. This is often called the color-TF relation. The same conclusions can be reached using either the 2MASS or I-band inclinations and different values of σ_i.

Figure 4 shows the value of the reduced χ^2 as a function of γ for the PP sample using the magnitude *k20fc* and an intrinsic scatter of 0.2mag. We find a minimum for each band: $\sim$ 0.5mag at J, $\sim$ 0.3 at H and $\sim$ 0.1 at K, although the amount of extinction at K is consistent with none. These curves are consistent with our results from the *cluster* sample, however, they are not fully reproduced when using the inclination from the I-band photometry. Our results are consistent with a reddenning of E(B-V) of 0.5 mag which gives a A_λ of 0.45mag, 0.28 and 0.18 for the three bands.

We did not see any correlation with type for the *cluster* data set while the PP data set shows a slight correlation. A linear fit gives a non-zero slope

---

[6] In order to find the proper keyword in the 2MASS data base, one need to add the prefix *j_m_*, *h_m_* or *k_m_* and the suffix *e* (*c*) for elliptical (circular) aperture.

[7] 2MASS has two kinds of magnitude type, "individual" (i20 & j21 here) and "fiducial"(k20f; j21f & kf here) . "Fiducial" means the aperture used for the photometry was selected at one band and applied to the other two.

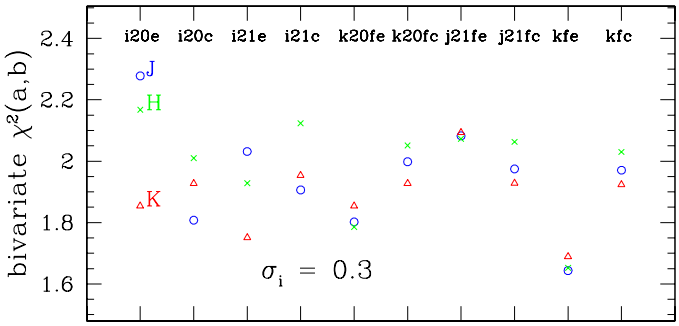

Figure 2. Top panel: For each of the magnitude types, the reduced χ^2 value of the fit is shown. For each of the magnitudes, the circles are for the J-band magnitude, the crosses are for the H-band, and the triangles are for the K-band. Circular (elliptical) aperture magnitudes are indicated the suffix c (e). Bottom panel: same as top panel using an intrinsic scatter σ_i of 0.3 mag. Both panels are for the *cluster* data set using 2MASS axis ratios for the inclination.

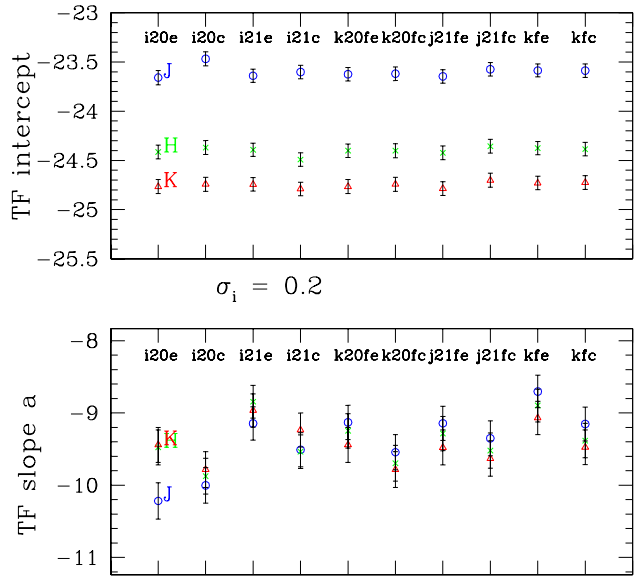

Figure 3. Top panel: Intercept of the TF fit for each of the magnitude types. For each of the magnitude, the circles are for the J-band magnitude, the crosses are for the H-band, and the triangles are for the K-band. Circular (elliptical) aperture magnitudes are indicated by the suffix c (e). Notice that the zero points are all within 1-σ of each other specially at K. Bottom panel: Slopes of the TF for each of the magnitude types. Both panels are for the *cluster* sub-sample using 2MASS axis ratios with no internal extinction correction.

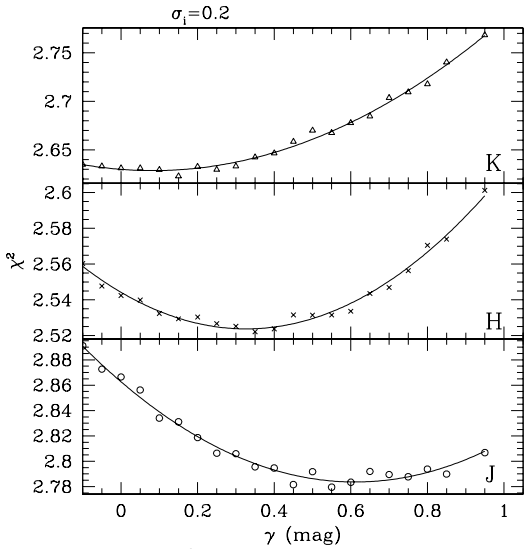

Figure 4. Plot of the χ^2_{min} as a function of the parameter γ for the PP data set. Each panel corresponds to J, H and K starting from the bottom. The open circle are the data points while the solid line is a fit of a second order polynomial. On sees the amount extinction (at the minimum of each curve) decreases as the wavelength increases as one would expect.

(-0.06) with 1-σ uncertainty of 0.03 for the PP data set, such that both results are consistent with no type dependence (at the 95% level).

We have not tested for dependence of the TF relation on surface brightness because the current 2MASS galaxy processor is not very sensitive to low surface brightness disks. Attemps are underway to extract them in the future.

5. Conclusions and discussions

Using our two samples (PP and *cluster* data sets), we found that using K-band is generally preferable over the other bands. The K-fiducial 20th mag/arcsec^2 (and the K-fiducial Kron[8]) seems to produce the least scatter. This is consistent with the K fiducial isophotal elliptical aperture magnitude being the most robust photometric measurement (Jarrett et al 2000). At low Galactic latitude, preliminary results suggests one would need optical axis ratios—The high star density can mislead the 2MASS ellipse-fitting program. The zero-point is well determined and is even independent of the magnitude types and of the sample. The TF slope shows more scatter but it steepens with wavelength. An interesting result is that we find internal extinction at each band, although the amount of extinction at K is consistent with none. We find no type dependence in our samples but we cannot yet conclude whether there is a surface brightness dependence.

[8]In the PP sample, the Kron K-fiducial does not produce such a low χ^2.

Our results are summarized below for the PP sample (equations 4 & 5) and the *cluster* sample (equations 6 & 7) using an intrinsic scatter of $\sigma_i = 0.2$ and assuming $\gamma = 0.1$mag of internal extinction.

$$M_K - 5\log h = (-9.90 \pm 0.35) \cdot (\log v_{rot} - 2.5) + (-24.70 \pm 0.10) \quad (4)$$
$$M_K - 5\log h = (-9.64 \pm 0.35) \cdot (\log v_{rot} - 2.5) + (-24.76 \pm 0.09) \quad (5)$$

Equations 4 & 6 are for the *k20fc* magnitude, while equations 5 & 7 are for the *k20fe* magnitude.

$$M_K - 5\log h = (-9.63 \pm 0.27) \cdot (\log v_{rot} - 2.5) + (-24.74 \pm 0.08) \quad (6)$$
$$M_K - 5\log h = (-9.58 \pm 0.29) \cdot (\log v_{rot} - 2.5) + (-24.86 \pm 0.10) \quad (7)$$

Both sample give very similar results.

As part of future work to study large scale flows in the ZOA, we have recently collected HI data at Arecibo for low Galactic latitude galaxies. Of 169 sources at $|b| < 10°$, 72 were detected; of 147 sources at $10° < |b| < 20°$ 75, were detected. The galaxies were identified using the 2MASS galaxy processor, which holds promise for identifying a large sample of galaxies within the ZOA.

Acknowledgments N. Bouché is the recipient of a Five College Astronomy Graduate Fellowship supported by the Mary Dailey Irvine Fund which allowed him to attend the meeting.

References

Bottinelli L., Gougueheim L., Fouqué P & Paturel G. 1990, A&AS, 82, 391

de Blok, W. J. G. & McGaugh, S. S. 1997, MNRAS, 290, 533

Giovanelli R., Haynes M.P., Herter T. & Vogt N. 1997, AJ, 113, 53

Huchtmeier W.K. & Richter O.G. 1989, A&A, 210, 1

Huchra J., Schneider S., Jarrett T., Chester T., Mader Jeff., Cutri R., Gizis J., Skrutskie M., Macri L., Rosenberg J., Steining R. 2000 in Mapping the Hidden Universe, ASP Conference Series (this volume), eds Kraan-Korteweg R.C., Henning P.A. and Andernach H.

Jarrett T.H., Chester T., Cutri R., Schneider S., Skrutskie N.& Huchra J.P. 2000, astro-ph/0004318 (AJ in press)

Koda J., Sofue Y. & Wada K. 1999, astro-ph/9907047 (ApJ submitted)

Koo, D.C. 1986, ApJ, 311, 651

Kron, R. G. 1980, ApJS, 43, 305

O'Neil K., Bothum G.D. & Schombert J. 2000, AJ, 119, 136O

Press W.H., Teukolsky S.A., Vetterling W.T. and Flannery B. 1992, *Numerical Recipes in C*, eds Cambridge University Press

Sakai S. et al 2000, ApJ, 529, 698

Steinmetz M. & Navarro J.F. 1999, ApJ, 513, 555

Tully B. & Fisher R. 1977, A&A, 54, 661

Tully B. & Fouqué P. 1985, ApJS, 58, 67

Zwaan M.A., van der Hulst J.M, de Blok W.J.G. & McGaugh S.S. 1995, MNRAS, 273, L35